Temporal evolution of the longitudinal- and transverse-phonon distributions in nonequilibrium metal films

N. Perrin
Laboratoire de Physique de la Matière Condensée de l'Ecole Normale Supérieure, 24 rue Lhomond, 75231 Paris CEDEX 05, France
and Université Pierre et Marie Curie, 4 Place Jussieu, 75252 Paris CEDEX 05, France

M. N. Wybourne
Materials Science Institute, University of Oregon, Eugene, Oregon 97403
(Received 18 December 1990)

We discuss the evolution of the nonequilibrium longitudinal- and transverse-phonon energy-density distributions in a thin metal film resulting from electron heating by the onset of an electric field. For a gold film on a sapphire substrate, we show that the ratio of the energy-density distributions for the T_1 and T_2 modes generated by longitudinal-phonon decay varies with time. The steady-state ratio is found to be a function of wave-vector magnitude; at high wave vectors it is determined by the relaxation rates for the spontaneous-phonon-decay processes in the film. We also find that the time taken for different parts of the energy-density spectra to reach their steady-state value depends on the magnitude of the phonon wave vector.

INTRODUCTION

Recently, transient-electron heating in metal films has been used to study the dynamics of nonequilibrium electron-phonon systems. Under ultrafast excitation conditions the electrons can exist out of equilibrium with the lattice for a time comparable to the electron-phonon relaxation time after which the electrons come to equilibrium with the lattice. This phenomenon has been observed by transient thermomodulation transmissivity[1,2] and femtosecond photoemission.[3] Other hot-electron effects have also been studied on this time scale, for example, electronic heat transport.[4] The electron energy relaxation that follows transient electron excitation has been exploited to generate phonons for the study of, for instance, thermal boundary resistance,[5,6] phonon focusing,[7] and phonon dynamics within thin films.[8] Two approaches have been used to describe the dynamics of the electrons and phonons. The first approach models the time evolution of the electron and phonon temperatures[9] which is valid at high temperatures where the phonon-phonon inelastic scattering is strong. The second approach was introduced by Perrin and Budd and treats the time evolution of the electron temperature and the phonon distribution.[10,11] This model is valid at lower lattice temperatures where the phonon-phonon interactions are insufficient to thermalize the phonon distribution. Both models use an electron temperature rather than an electron distribution. When comparing the models to most experimental results this is a good approximation because the typical excitation power densities provide high transient-electron temperatures for which the electron-electron scattering is sufficiently rapid to thermalize the electron distribution.

We have recently extended the Perrin and Budd model to include the effects of anharmonic three-phonon processes on the temporal evolution of the longitudinal-phonon distribution within a metal film.[12–14] In this paper we present results for the temporal evolution of the transverse-phonon spectra in the presence of anharmonic processes. We will assume the film to be fabricated from a simple metal with a spherical Fermi surface, and we will ignore the possibility of umklapp processes. Furthermore, we will assume the metal is clean, that is, $ql > 1$ where q is the phonon wave-vector magnitude and l is the elastic mean free path of the electrons. Within these approximations the only method to generate transverse phonons in the excited film is by energy relaxation of the longitunal phonons by spontaneous three-phonon processes. The three-phonon processes that produce the T_1 and T_2 modes have different relaxation rates, which together with the fact that there are two channels for decay to T_2 yet only one for T_1, gives different evolutions of the two modes.

MODEL

To analyze the generation of phonons we follow our previous work[12–14] and assume the phonon and electron distributions to be spatially uniform. In this approximation the evolution of the nonequilibrium longitudinal-phonon distribution $N_L(q)$ for wave-vector magnitudes $q > q_{ZB}/2$ is found by evaluating

$$\frac{\delta N_L(q)}{\delta t} = \frac{\bar{N}_L(q,T_e) - N_L(q)}{\tau_{e\text{-ph}}(q)} + \frac{\bar{N}_L(q,T_0) - N_L(q)}{\tau_x(q)} , \tag{1}$$

where q_{ZB} is the wave-vector magnitude at the zone boundary.

For wave vector magnitudes $q \leq q_{ZB}/2$ an extra term, $-\{[\bar{N}_L(2q,T_0)-N_L(2q)]/\tau_1(2q)\}$ must be added to include the generation of longitudinal phonons from the three-phonon process. In these expressions T_e and T_0 are the electron and substrate temperature, respectively, and $\bar{N}_j(q,T)$ is the Bose distribution of mode j evaluated at temperature T and wave vector q. The scattering rate $\tau_x^{-1}(q)$ is given by

$$\tau_x^{-1}(q)=(\tau_b^L)^{-1}+\tau_1^{-1}(q)+\tau_2^{-1}(q)+\tau_3^{-1}(q) ,$$

where $(\tau_b^L)^{-1}$ is the phonon escape rate from the film and the relaxation rates $\tau_1^{-1}(q)$, $\tau_2^{-1}(q)$, and $\tau_3^{-1}(q)$ describe the three possible anharmonic processes in an isotropic solid, $L \rightarrow L+T_2$, $L \rightarrow T_1+T_1$, and $L \rightarrow T_2+T_2$, respectively. The phonon escape rate has been taken to be of the usual, frequency-independent form $(\tau_b^j)^{-1}=v_j/4\eta d$ where v_j is the sound velocity of mode j, d is the film thickness, and η is an acoustic mismatch parameter.[15,16] Within the Debye approximation the relaxation rates for the anharmonic processes have been shown to be proportional to q^5.[17] Recently, Berke, Mayer, and Wehner[18] presented explicit expressions for $\tau_1^{-1}(q)$, $\tau_2^{-1}(q)$, and $\tau_3^{-1}(q)$ which we have used in this work. We note the collinear process $L \rightarrow L+L$ is also possible:[19] we neglect it in the present calculation since the decay rate is small compared with the other processes. Transverse-phonon decay should not be considered since it is prohibited in an isotropic solid because of the conditions of energy and momentum conservation. In the clean metal limit the electron-phonon relaxation rate is given by[20]

$$\tau_{e\text{-ph}}^{-1}=\frac{\Xi^2 m^2 q}{2\hbar^3 \pi \rho_D} ,$$

where Ξ is the deformation potential, m is the electron mass, and ρ_D is the mass density of the film.

To obtain the phonon spectrum, the variation with time of the electron temperature must be simultaneously calculated. This is done by evaluating the equation

$$C_e\frac{dT_e}{dt}=\frac{E^2}{\rho}-\sum_{\mathbf{q}}\hbar\omega(q)\left[\frac{\bar{N}_L(q,T_e)-N_L(q)}{\tau_{e\text{-ph}}(q)}\right] , \quad (2)$$

where C_e is the specific heat of the electrons (γT_e), E is the applied electric field, and ρ is the resistivity of the film.

The evolution of the transverse-phonon spectrum can be described in a similar fashion to that of the longitudinal phonons except there is no generation from the electrons, rather the generation comes only from down conversion. The corresponding equation for the T_1 mode is

$$\frac{\delta N_{T_1}(q)}{\delta t}=-\frac{2\left[\bar{N}_L\left[\frac{2q}{c},T_0\right]-N_L\left[\frac{2q}{c}\right]\right]}{\tau_2\left[\frac{2q}{c}\right]}+\frac{\bar{N}_{T_1}(q,T_0)-N_{T_1}(q)}{\tau_b^{T_1}} , \quad (3)$$

where $q \leq q_{ZB}/2$ and $c=v_L/v_T$. The factor of 2 accounts for the number of phonons generated in the decay process $L \rightarrow T_1+T_1$.

Similarly for the T_2 mode we have

$$\frac{\delta N_{T_2}(q)}{\delta t}=-\frac{\bar{N}_L\left[\frac{2q}{c},T_0\right]-N_L\left[\frac{2q}{c}\right]}{\tau_z\left[\frac{2q}{c}\right]}+\frac{\bar{N}_{T_2}(q,T_0)-N_{T_2}(q)}{\tau_b^{T_2}} , \quad (4)$$

where $\tau_z^{-1}(2q/c)=\tau_1^{-1}(2q/c)+2\tau_3^{-1}(2q/c)$ and so the first term represents phonons generated by two parallel down-conversion processes. Again the factor of 2 accounts for the number of phonons generated in the decay process $L \rightarrow T_2+T_2$.

DISCUSSION

We have used the model to calculate the evolution of the longitudinal and transverse phonon spectra generated by the excitation of a 10-nm-thick gold film on sapphire. The equilibrium substrate temperature was taken to be $T_0=7$ K. The following constants were used in our calculation: electron density $n=6\times10^{28}$ m^{-3}, $\rho=5\times10^{-8}$ Ω m, $\rho_D=19\,300$ kg m^{-3}, and $\Xi=3.77$ eV. From the elastic constants discussed in our earlier paper[12] we estimate the velocities of sound in gold to be $v_L=3.42\times10^3$ m s^{-1} and $v_T=1.32\times10^3$ m s^{-1}. With these parameters, and $\eta=12.5$, we calculate the rates of phonon escape from the film to the substrate to be $(\tau_b^L)^{-1}=0.68\times10^{10}$ s^{-1} and $(\tau_b^{T_1})^{-1}=(\tau_b^{T_2})^{-1}=0.26\times10^{10}$ s^{-1}. We have also estimated the relaxation rates for the three-phonon processes to be $\tau_1^{-1}(q)=7\times10^{-41}q^5$ s^{-1}, $\tau_2^{-1}(q)=2\times10^{-40}q^5$ s^{-1}, and $\tau_3^{-1}(q)=4\times10^{-40}q^5$ s^{-1} indicating that the $L \rightarrow T_2+T_2$ is the dominant anharmonic decay process for the longitudinal phonons. Finally, the magnitude of the zone-boundary wave vector was estimated from the fcc structure of gold and the low-temperature lattice constant of 0.395 nm, to be 1.72×10^{10} m^{-1}.

Numerical convergence of the phonon spectra was checked by using several different time intervals in the calculations. Convergence to better than 1% was achieved when the interval was reduced below $\sim10^{-2}$ the value of the fastest phonon relaxation process.

The evolution of the longitudinal- and transverse-phonon (T_2) energy density distributions, $q^3N_L(q)$ and $q^3N_{T_2}(q)$, generated after an electric field of 1.55×10^5 V m^{-1} was applied to the film, are shown in Figs. 1 and 2, respectively. For wave vectors close to the zone center, $(\tau_b^L)^{-1} > \tau_{e\text{-ph}}^{-1} > \tau_3^{-1}$; so the longitudinal phonons are generated less rapidly than they can escape and they do not undergo any anharmonic processes. Therefore, at all times the energy density distributions for small wave-vector magnitudes remain very close to the distributions characterized by the substrate temperature. For

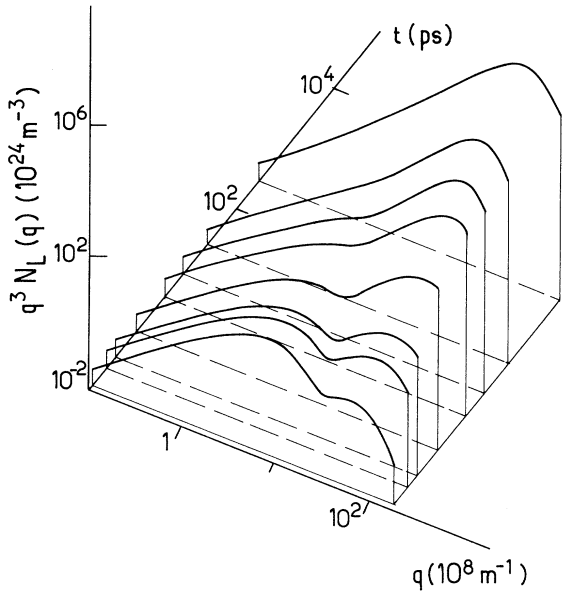

FIG. 1. Evolution of the longitudinal-phonon energy density distribution for an electric field $E=1.55\times10^5$ V m^{-1}. The origin of the axes corresponds to $q=10^{-7}$ m^{-1}, $t=10^{-1}$ ps, and $q^3N_L(q)=10^{-2}\times10^{24}$ m^{-3}.

wave vectors above $\sim q_{ZB}/2$, $(\tau_b^L)^{-1}<\tau_{e\text{-ph}}^{-1}<\tau_3^{-1}$ so the longitudinal phonons generated by electron relaxation rapidly decay before escaping the film. The fastest relaxation time for the three-phonon process is $\tau_3(q_{ZB})=1.7$ ps. Consequently, at times less than 1.7 ps, the energy density distribution for the longitudinal phonons shows a pronounced increase above $q_{ZB}/2$ while the distribution for the T_2 modes is largely unaffected. At times greater than 1.7 ps, decay to T_2 phonons becomes very probable as seen by the increased energy density for the T_2 mode at the zone boundary (Fig. 2). It is interesting to note that electron-phonon relaxation occurs preferentially via large wave-vector phonons yet we do not observe a maximum of the longitudinal-phonon energy density at the zone boundary for any times after excitation. The reason for this is that $\tau_{e\text{-ph}}^{-1}(q_{ZB})<\tau_3^{-1}(q_{ZB})$ so that any near-zone-boundary phonons generated have a high probability of decay.

One consequence of the different decay processes for the generation of T_1 and T_2 phonons is that the evolution of the energy density distribution of the two modes is different. To illustrate this we have plotted in Fig. 3 the ratio N_{T_1}/N_{T_2}, as a function of wave vector, for different times after excitation. Before excitation the ratio is unity and simply reflects the ratio of the equilibrium distributions at 7 K. Since $\tau_z^{-1}>\tau_2^{-1}$, after excitation the energy density distribution of the T_2 mode increases more rapidly than that of the T_1 mode for phonons near the zone boundary. Thus the ratio is reduced. The reduced ratio moves towards lower wave-vector magnitudes as time increases, with the ratio limiting to $N_{T_1}/N_{T_2}\sim0.46$. The origin of this limiting value can be deduced from Eqs. (3) and (4). When the longitudinal phonons are significantly heated, so that $N_L(2q/c) \gg \bar{N}_L(2q/c,T_0)$ and $N_{T_i}(q)\gg\bar{N}_{T_i}(q,T_0)$ $(i=1,2)$ the ratio is independent of q and is given by

$$\frac{N_{T_1}}{N_{T_2}}\approx\frac{2\tau_b^{T_1}}{\tau_2\left[\frac{2q}{c}\right]}\frac{\tau_z\left[\frac{2q}{c}\right]}{\tau_b^{T_2}}=\frac{2\tau_z\left[\frac{2q}{c}\right]}{\tau_2\left[\frac{2q}{c}\right]}=0.46\ .$$

The shift of the reduced ratio towards lower wave vectors

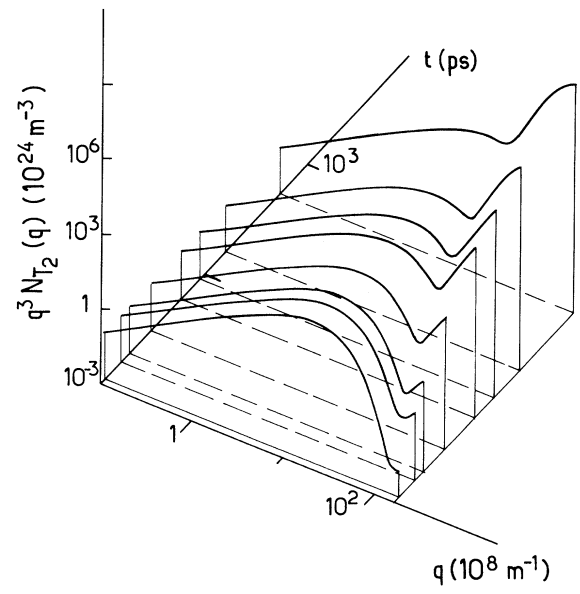

FIG. 2. Evolution of the transverse-phonon energy density distribution for an electric field $E=1.55\times10^5$ V m^{-1}. The origin of the axes corresponds to $q=10^{-7}$ m^{-1}, $t=10^{-1}$ ps, and $q^3N_{T_2}(q)=10^{-3}\times10^{24}$ m^{-3}.

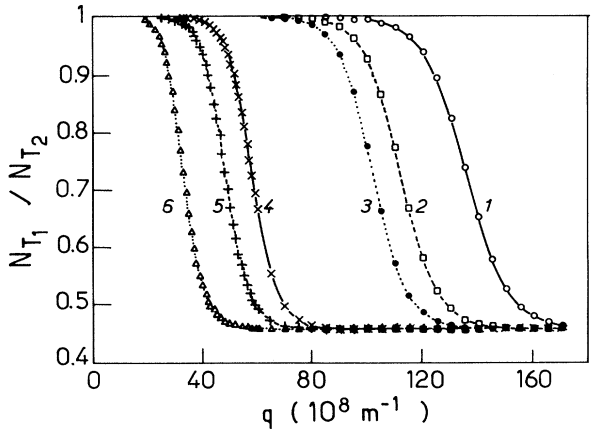

FIG. 3. Ratio N_{T_1}/N_{T_2} as a function of wave vector q for different times t after excitation; t (ps): (1) 0.125; (2) 0.25; (3) 0.375; (4) 8.75; (5) 26.25; (6) 301.25.

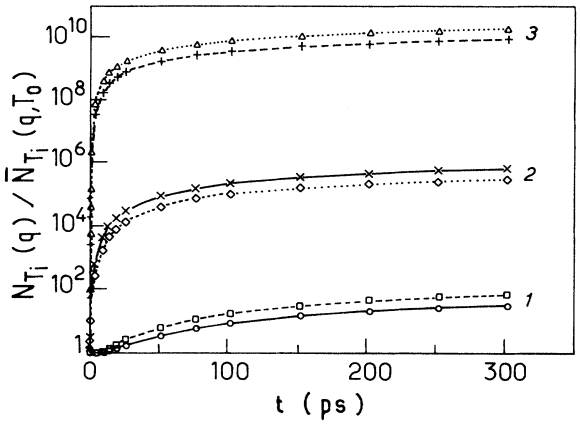

FIG. 4. Ratio $N_{T_i}(q)/\bar{N}_{T_i}(q,T_0)$ as a function of time t ($i=1$, lower curves; $i=2$, upper curves) for three different wave vectors: (1) $q=50\times10^8$ m^{-1}; (2) $q=100\times10^8$ m^{-1}; (3) $q=q_{ZB}$.

eventually ceases as the steady state is approached. This is seen in Fig. 3 in which curve 6 corresponds to the steady state. The transition between $N_{T_1}/N_{T_2}=1$ and $N_{T_1}/N_{T_2}=0.46$ in the steady state occurs at approximately $q=30\times10^8$ m^{-1}. We can understand this by comparing the generation and escape rates for the longitudinal phonons. At wave vectors below 30×10^8 m^{-1}, the generation rate is smaller than the escape rate.

In order to determine the time taken by different parts of the spectra $q^3N_{T_1}(q)$ and $q^3N_{T_2}(q)$ to come to their steady-state value, we followed the time response for three different wave vectors, 50×10^8 m^{-1}, 100×10^8 m^{-1}, and q_{ZB}, as shown in Fig. 4. The time taken to reach the steady-state value of the phonon energy density clearly increases with decreasing wave vector while both modes appear to reach the steady-state value in approximately the same time. This can be understood by considering the relaxation rates τ_1^{-1}, τ_2^{-1}, and τ_3^{-1}. The two highest rates are τ_3^{-1} describing the $L\rightarrow T_2+T_2$ process and τ_2^{-1} describing the $L\rightarrow T_1+T_1$ process. The ratio τ_3^{-1}/τ_2^{-1} is independent of q and equals 2. Therefore, for all wave vectors the two modes are expected to reach their steady-state value in approximately the same time. However, since the relaxation rates are proportional to q^5, the decay of longitudinal phonons having wave vectors smaller than q_{ZB} to produce the transverse phonons of low q will be less likely. Thus N_{T_1} and N_{T_2} away from q_{ZB} will take longer to reach a steady state. Finally, we note that the steady-state ratio $N_{T_1}/N_{T_2}\sim0.46$ is clearly seen for all three wave vectors.

CONCLUSION

We have shown how the longitudinal- and transverse-phonon distributions in a thin gold film evolve after electron heating. At a particular phonon wave vector, the ratio of the energy densities for the T_1 and T_2 modes varies with time and comes to a steady-state value that is determined by the relaxation rates.

ACKNOWLEDGMENTS

This work was supported by a grant from NATO. Part of this work was supported by the National Science Foundation under Grant No. DMR 87-13884.

[1]H. E. Elsayed-Ali, T. B. Norris, M. A. Pessot, and G. A. Mourou, Phys. Rev. Lett. **58**, 1212 (1987).
[2]R. W. Schoenlein, W. Z. Lin, J. G. Fujimoto, and G. Eesley, Phys. Rev. Lett. **58**, 1680 (1987).
[3]J. G. Fujimoto, J. M. Liu, E. P. Ippen, and N. Bloembergen, Phys. Rev. Lett. **53**, 1837 (1984).
[4]S. D. Brorson, J. G. Fujimoto, and E. P. Ippen, Phys. Rev. Lett. **59**, 1962 (1987).
[5]R. Stoner, D. A. Young, H. J. Maris, J. Tauc, and H. T. Grahn, in *Phonons 89*, edited by S. Hunklinger, W. Ludwig, and G. Weiss (World Scientific, Singapore, 1990), p. 1305.
[6]E. T. Swartz and P. O. Pohl, Rev. Mod. Phys. **61**, 605 (1989).
[7]J. P. Wolfe, in *Phonons 89*, edited by S. Hunklinger, W. Ludwig, and G. Weiss (World Scientific, Singapore, 1990), p. 1335.
[8]M. N. Wybourne, J. K. Wigmore, and N. Perrin, J. Phys. Condens. Matter **1**, 5347 (1989).
[9]S. I. Anisimov, B. L. Kapeliovich, and T. L. Perelman, Zh. Eksp. Teor. Fiz. **66**, 776 (1974) [Sov. Phys. JETP **39**, 375 (1975)].
[10]N. Perrin and H. Budd, Phys. Rev. Lett. **28**, 1701 (1972).
[11]N. Perrin and H. Budd, J. Phys. (Paris). Colloq. **33**, C4-3 (1972).
[12]N. Perrin, M. N. Wybourne, and J. K. Wigmore, Phys. Rev. B **40**, 8245 (1989).
[13]N. Perrin, M. N. Wybourne, and J. K. Wigmore, in *Phonons 89*, edited by S. Hunklinger, W. Ludwig, and G. Weiss (World Scientific, Singapore, 1990), p. 811.
[14]M. N. Wybourne and N. Perrin, Phys. Rev. B **42**, 11 345 (1990).
[15]W. A. Little, Can. J. Phys. **37**, 334 (1959).
[16]O. Weis, Z. Angew. Phys. **26**, 325 (1969).
[17]S. Tamura, Phys. Rev. B **31**, 2575 (1985).
[18]A. Berke, A. P. Mayer, and R. K. Wehner, J. Phys. C **21**, 2305 (1988).
[19]S. Simons, Proc. R. Soc. London **82**, 401 (1963).
[20]A. B. Pippard, Philos. Mag. **46**, 1104 (1955).